NAST-I for Air Quality Monitoring and Wildfire-Related Research

Daniel K. Zhou, Allen M. Larar, Xu Liu, Xiaozhen Xiong, and Hyun-sung Jang
NASA Langley Research Center, Hampton, VA 23681

Acknowledgment:
Bill Smith, Sr. (HU & UW), Jake Kaye (NASA), Mitch Goldberg (NOAA), and Many Others …

Introduction

The National Airborne Sounder Testbed-Interferometer (NAST-I) is an airborne FTS remote sensor that nominally flies on NASA high-altitude aircraft to serve as a spaceborne instrument simulator. NAST-I continues to serve as a pathfinder for future satellite FTS systems and the next generation advanced atmospheric sounders in general. NAST-I provides high resolution spectrally resolved infrared radiances as its level-1 product. NAST-I level-2 products characterizing the surface (i.e., skin temperature and spectral emissivity), atmosphere (i.e., profiles of temperature, moisture, ozone, carbon monoxide, and other trace species), and clouds (e.g., optical depth, particle size, temperature, and height) can be used to support fire-related monitoring and research. NAST-I provided 3-d characterizations of wildfire-induced plumes of CO during the FIREX-AQ field campaign (conducted during 2019) which showed the intensity and size evolution of wildfire plumes at high spatial and temporal resolutions. Wildfire-induced CO plumes, in conjunction with their evolution, transport, and age have been identified and recently published in scientific journals. Other research applications, such as surface emissivity changes due to fire burning of ground landscape, have been under investigation. These NAST-I level 1-3 products could be used in support of wildfire management to better inform decision making and operations for pre-, active, and post-fire environments.

NAST-I: Brief Description and Objectives

NAST-I was developed in 1997-1998; refurbished in 2009 & 2016.

NAST-I Sensor Characteristics:
- Michelson interferometer (FTE).
- ~8500 spectral channels, ~650-2800 cm^{-1} at 0.25 cm^{-1} spectral resolution.
- Spatial resolution ~130 m/km flight altitude.
- Radiances ~0.5 K absolute accuracy with 0.1 K precision.

Aircraft Accommodation:
- ER-2 wing super pod
- PROTEUS underbelly pod
- WB-57 underbelly pallet.

NAST-I Field Campaigns:
- Before AIRS launch (<2002): 9 missions collecting geophysical field state characterization for satellite remote sensing system risk mitigation (sensors and algorithms).
- After AIRS launch (>2002): 13 missions for advanced satellite remote sensor Cal/Val (e.g., Aqua AIRS, MetOp IASI, & SNPP/JPSS CrIS), and airborne science.
- The most recent field campaign: FIREX-AQ (August 2019).

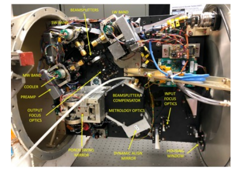

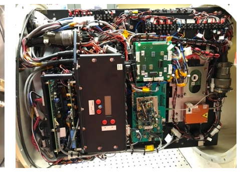

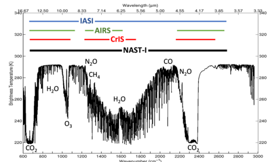

NAST-I spectral coverage encompasses all satellite IR sounders with a higher (or equivalent) spectral resolution and higher spatial resolution.

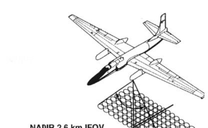

NAST-I Level 2 Data Processing

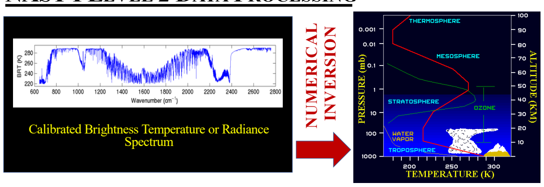

Retrievals under cloudy conditions:
- Atmospheric profile through optically thin cirrus clouds and above optically thick clouds.
- Effective cloud parameters.

Retrievals under clear conditions:
- Surface skin temperature and emissivity.
- Atmospheric temperature and moisture profiles; and atmospheric CO and O_3 profiles.

Tracking Active Fire with Remoted-sensed Surface Emissivity

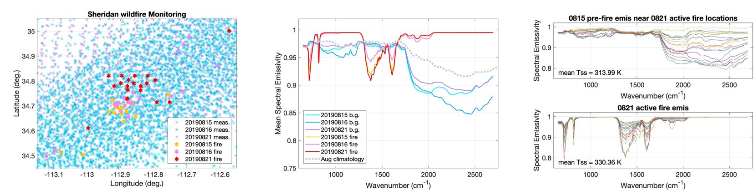

Preliminary Result: Active Sheridan fire location detected by NAST-I emissivity from the flights of August 15 to 16, then to 21, 2019. Sheridan fire spreads in north-east direction during this period.

Sheridan Fire Induced CO Distribution and Evolution

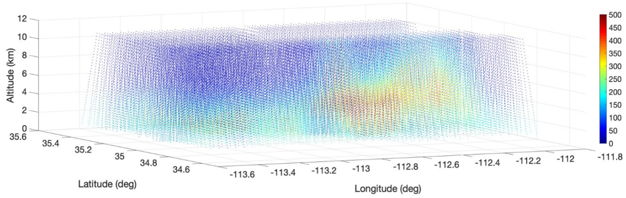

NAST-I three-dimensional CO (ppb) distribution shows the plume evolution and transport near the Sheridan fire ground location (34.80º latitude, -112.85º longitude) from August 21, 2019.

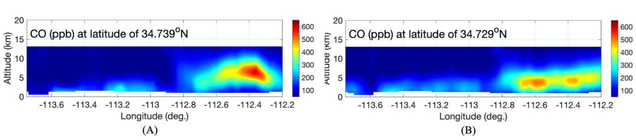

CO time-evolution shown in its vertical profile cross sections up- and down-wind of the Sheridan fire location (about 140 km) from (A) 23:28:13–23:39:37 UTC of August 21, 2019, to (B) 00:38:35–00:49:24 UTC of August 22, 2019. (A) and (B) are about 70 minutes apart.

Williams Flats Fire Induced CO Plume Progression

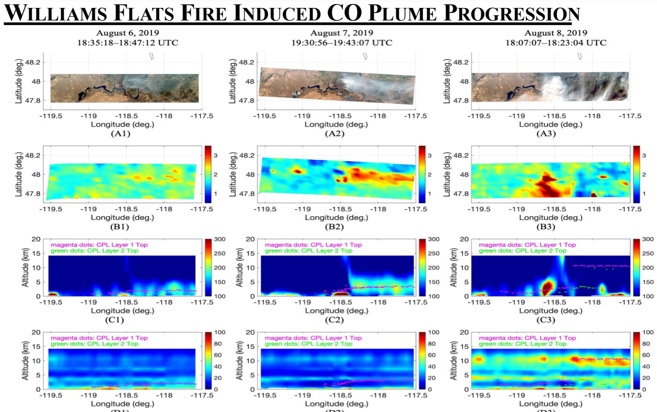

Williams Flats fire progression from August 6 (left column), to August 7 (middle column), then to August 8 (right column). (A) eMAS true-color imageries, (B) CO column density (10^{18}/cm^2), (C) CO vertical profile (ppb) cross section with CPL layer top, and (D) the relative humidity vertical profile (%) cross section with CPL layer top.

Wildfire CO Plume Age Estimation

Wildfire plume age is estimated using O_3 and CO data based on an empirical relationship derived from in-situ measurements*. A positive relationship is found between the $\Delta O_3/\Delta CO$ ratio and plume age.
For this case study of wildfire plume age, we have chosen the ER-2 sorties over the William Flats fire and the extended downwind area from August 7, 2019, as the ER-2 sorties have ~450 km downwind flight leg segments

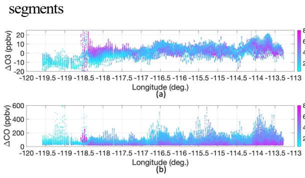

(a) ΔO_3 and (b) ΔCO distribution within the fire-induced plumes.

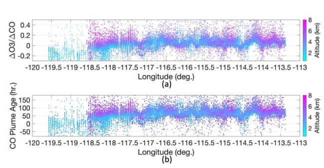

$\Delta O_3/\Delta CO$ distribution along the longitude within the fire-induced plumes, and (b) estimated plume age distribution.

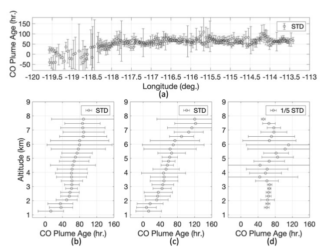

(a) Plume age distribution along the longitude. Plume age distribution along the altitude: (b) all data shown from (a), (c) data from longitude less than -117.0º (near fire location), and (d) data from longitude greater than -117.0º (further away from fire location.

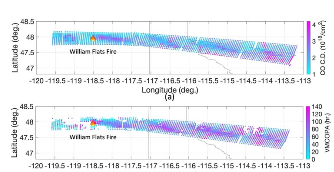

Distribution of (a) CO column density and (b) vertical mean CO plume age (VMCOPA).

*D. A. Jaffe and N. L. Wigder, "Ozone production from wildfires: A critical review," *Atmospheric Environment*, **51**, 1-10 (2012).

Conclusion

- Wildfire induced CO plumes, in conjunction with their evolution and transport, are readily identified with NAST-I measurements.
- NAST-I retrieval ability is demonstrated showing the contrast between nominal atmospheric background and fire-induced elevated CO profiles.
- NAST-I remotely-sensed CO and O_3 are evaluated by favorable inter-comparisons with the in-situ CO and O_3 measurements which show a positive agreement (not shown here).
- Plume characterization correlation between CO and smoke-dust detected by the CPL and eMAS is assessed and presented a good correspondence.
- Elevated tropospheric CO induced by the wildfire is associated and correlated with the total carbon emission from biomass burning (not shown here).
- Plume age estimation in a 3-d high-spatial-resolution adds critical temporal information of the fire-induced plume, demonstrating the capability of an ultraspectral remote sensor with a higher spectral and spatial resolution to monitor CO and O_3 and its advantage of giving broader spatial and temporal assessment by rapidly covering a large field of observation.
- Active fire location is identified by remote-sensed surface emissivity and can be tracked to monitor its movement.

Reference:

Zhou, D. K., A. M. Larar, X. Liu, A. M. Noe, G. S. Diskin, A. J. Soja, G. T. Arnold, and M. J. McGill (2021), Wildfire-induced CO plume observations from NAST-I during the FIREX-AQ field campaign, *IEEE J. Sel. Topics Appl. Earth Observ. Remote Sens.*, **14**, 2901–2910.

Jaffe D. A. and N. L. Wigder (2012), Ozone production from wildfires: a critical review, Atmos. Environ., **51**, 1–10.

Zhou, D. K. A. M. Larar, X. Liu, and X. Xiong (2022), Estimation of wildfire-induced CO plume age from NAST-I measurements during FIREX-AQ field campaign, *J. Appl. Remote Sens.*, **16**(3), 034522.